

Study on phase transition heat transfer of nanofluids in porous media based on LBM

Tongtong Li^{1, a}, Yunfei Ji^{1, a}, and Ke Li^{1, a *}

¹School of Energy and Environment, Inner Mongolia University of Science and Technology, Baotou 14010, China;

^akelitsinghua@163.com

Abstract. In this paper, a lattice Boltzmann method is used to simulate the phase transition heat transfer of nanofluid in a miniature heat tube in a porous medium. Based on this, the existing research basis is summarized, the influence of nanoparticles on the thermal properties of the base solution is analyzed, the relevant thermal property prediction model is constructed, and the thermal property parameters of nanofluid are fitted. We generated porous media with different porosity with particle size of 100 micron to 150 microns. Combining the force form proposed by Gong with the exact difference method, the interparticle force is introduced. Based on the improved LBM model and the coupled energy equation, so as to analyze the phase transition heat transfer situation of nanofluids with different thermal properties in porous media. The study shows that nanofluidics can effectively enhance the heat transfer performance of heat pipe equipment. In a certain concentration limit, with the increase of volume concentration, the heat transfer performance of heat pipe is enhanced. The greater the temperature difference between the cold and heat source, that is, the higher the temperature of the heat source, the lower the cold source temperature, the better the heat transfer performance of the heat pipe. For the fluid flow in the porous media region, that is, the turbulent phenomenon that may occur in the porous media, and more vortices occur in the porous media with 40% and 50% porosity. Higher porosity has better heat pipe temperature uniformity.

Keywords: Lattice Boltzmann method; Nanofluids; Porous medium heat pipe; Phase change heat transfer

1. Introduction

With the rapid development of microelectronics technology, the heat load carrying capacity of equipment is increasing day by day, and the demand for micro-scale heat transfer in various countries is also increasing year by year. The electronic device will release a large amount of heat during its operation. If the heat is not transmitted in time during the operation of the device, the electronic components will be damaged. In the past, equipment with blade auxiliary equipment is often used for heat transfer, but this method will take up a lot of space, which is not conducive to the installation and use under specific circumstances. It is of internal value to carry out heat transfer research.

Boltzmann is a method to study the fluid flow and heat transfer process. It uses distribution functions to study the continuity and dispersion of the fluid and the macroscopic and microscopic relations. It has significant advantages in handling complex boundary conditions, and is widely used in microscale heat transfer and mass transfer, and multiphase flow simulation [1-11].

2. Theoretical model

2.1 Nanofluid

As shown in Figure 2.1, due to the obvious transscale characteristics of nanofluids, nanoparticles in the base solution are influenced by Brownian motion, agglomeration, penetration, thermophoresis, radiation heat transfer, charge adsorption and repulsion, and the energy transfer is very complex, so the analysis of the thermal conductivity mechanism of nanofluidics is particularly important [12].

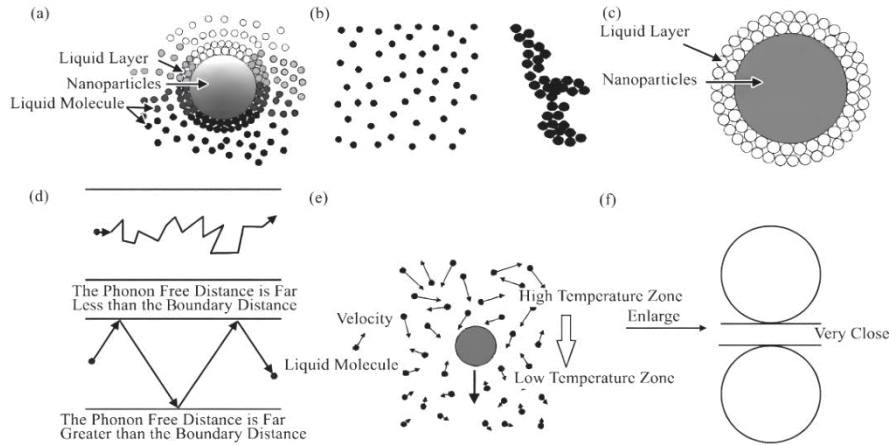


Figure 2.1 Mechanism of the heat transfer of nanoparticles

Based on the model of thermal conductivity, viscosity, density and specific heat capacity of nanofluid, the factors that may affect the thermal property of nanofluid are analyzed, and the thermal conductivity of nanofluid decreases with the increase of particle size, and the decrease decreases with the increase of particle size. And increased with increasing concentration. When the temperature of the fluid increases, the thermal conductivity of the base solution will increase; the Brownian motion of the nanoparticles in the liquid will become intense, which gives the prediction of the model.

2.2 Boltzmann method

Multiphase flow generally exists in all kinds of heat exchange equipment, and its research has been widely concerned by scholars in many countries. In order to analyze and simulate the data and effect of the heat transfer efficiency of heat transfer equipment quickly and accurately, the level of modern computational fluid technology is also improving day by day, on which various computational fluid simulation methods are born, among which the lattice Boltzmann method has become a very effective fluid simulation method after more than 30 years of development.

D2Q9 model was used to complete the simulation, and the specific construction process for this following. As shown in Figure 2.2, the two-dimensional space is discretized into squares, and the eight nodes in the outer layer of the model are regarded as adjacent nodes. At any time step, particles migrate to adjacent nodes. In the next collision, it will collide in the form of new particles and migrate to adjacent nodes. Each node in the D2Q9 model [13] has three different state particles: static, vertical direction motion, and diagonal direction motion, with a speed configuration of:

$$e_a = \begin{cases} (0,0) & a = 0 \\ \sqrt{2}c \left\{ \cos \left[(2a - 1) \frac{\pi}{4} \right], \sin \left[(2a - 1) \frac{\pi}{4} \right] \right\} & a = 5,6,7,8 \\ \sqrt{2}c \left\{ \cos \left[(2a - 1) \frac{\pi}{4} \right], \sin \left[(2a - 1) \frac{\pi}{4} \right] \right\} & a = 5,6,7,8 \end{cases}$$

Where $c = \delta_x / \delta_t$ is the unit speed, δ_x and δ_t for the time step and grid step, in general $\delta_x = \delta_t$.

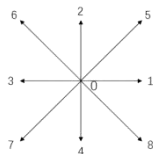


Figure 2.2 D2Q9 model speed configuration

In this paper, we combine the action force form proposed by Gong with the exact difference method, and establish a dual distribution function model based on the improved LBM model.

Secondly, the relationship between porosity and permeability of porous media was analyzed, and random functions were used to generate porous media with different porosity of particle size of 100 micron to 150 micron, and then the thermal property parameters of fluid were set to lay a theoretical foundation for fluid simulation.

2.3 Modelling verification

The simulation involves the phase change heat transfer process. In order to obtain the coexistence curve of saturated liquid phase and saturated gas phase, the P-REO equation and Maxwell construction are used for model verification, as shown in Figure 2.3 and Figure 2.4. In Figure 2.3, the P-REOS equation coexistence curve[14] obtained from the Gong[15] is compared with the Maxwell construction in Figure 2.4. The P-REOS equation uses the fluid saturation temperature used for the fluid gas-liquid density ratio; the ink point in the Maxwell construction diagram represents the simulation value of the proposed model, and the smooth curve is the Maxwell construction structure curve, which well fits the Maxwell construction theory solution, thus verifying that the model used in this paper is accurate and reliable.

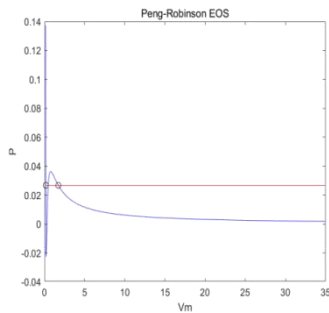


Figure 2.3 P-R EOS equation for solving Fig

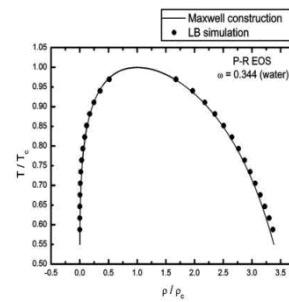


Figure 2.4 Maxwell construction

The whole phase conversion thermal process is performed in the 2000*400 calculation domain:

The $y \leq 150$ in the calculation domain is the porous medium and the liquid, and the part of the $y \geq 150$ is the water vapor. Heat pipe $x \leq 200$ is the evaporation end, and the heat source $T = 1.2 * T_c$ is applied to the bottom; Heat pipe $x \leq 1200$ is the condensing end, apply the cold source $T = 0.8 * T_c$ at the bottom; The heat pipe 200×1200 is the adiabatic end, and the equilibrium temperature at the bottom is $T = 1.0 * T_c$. The boiling temperature of the fluid is $T_s = 0.9 * T_c$.

Other fluid thermoproperties and lattice scale coefficients are shown in Table 4.1 [16].

Table 4.1 Table of simulated important parameters

Physical name	Actual physical quantity	Grid unit volume
The lattice length	0.000025m	1
Density of liquid phase	713.97kg/m ³	5.9
Density of gas phase	70.18kg/m ³	0.58
Liquid phase viscosity	0.0000826Pa · s	0.354
Air phase viscosity	0.0000201Pa · s	0.086
The liquid-phase thermal diffusion coefficient	0.000000247m ² /s	0.129
Gas-phase thermal diffusion coefficient	0.000000356m ² /s	0.185
critical temperature	647.3K	0.072922
critical density	322kg/m ³	2.66091
Thermal conductivity of the nanoparticles	237W/(m*k)	Null
Nanoparticle density	2700kg/m ³	Null
Specific heat capacity of the nanoparticles	880J/(kg*k)	Null

3. Analysis of influencing factors

This chapter uses the porous medium structure generated by the stochastic function method, combined with the constructed Boltzmann model and the coupled energy equation to study the enhanced heat transfer effect of nanofluidics on the heat tube, using the idea of control variables. The influence of heat source temperature and porous medium on the flow of fluid in the porous medium is analyzed quantitatively.

3.1 The effect of different heat source temperatures on heat transfer

To study the effect of the heat source temperature on the heat transfer performance of the heat pipe, this paper simulated the corresponding change of the average wall temperature at the evaporation end and the condensing end of the 1% volume nanofluid under the same boundary conditions and different heat source temperature.

Here, four sets of temperatures are set for comparative analysis. The heat source temperature is $1.20T_c$, $1.25T_c$, $1.30T_c$, $1.35T_c$, and the cold source temperature is always $0.80 T_c$, and the temperature difference gradually increases. The average wall temperature at the evaporation end and the condensing end was analyzed separately, analyzing a set of data for every 100 time steps for 0.4 seconds and every 200 time steps after 0.4 seconds, as shown in Figure 3.1.

As can be seen from Figure 3.1, at the beginning of heat transfer, the temperature difference of the fourth group is largest, and the average wall temperature of the evaporation end increases the most rapidly. After temperature stabilization, the stable average wall temperature of the evaporation end of the heat pipe using nanofluid is lower than that of the base solution. Comparing the simulation results of the four groups, it can be found that as the temperature difference of the initial conditions gradually increases, the highest temperature of the average wall of the evaporation end will also increase, and the comprehensive heat transfer performance of the heat pipe is enhanced. The average wall temperature of the condensing end of the heat tube using nanofluidics is higher than enabling use a basic solution. This indicates that the heat tube using nanofluidics conducts the heat most rapidly, and at the same cold source temperature, the condensing end fluid can be liquefied and release heat most rapidly, and transfer the heat to the natural environment.

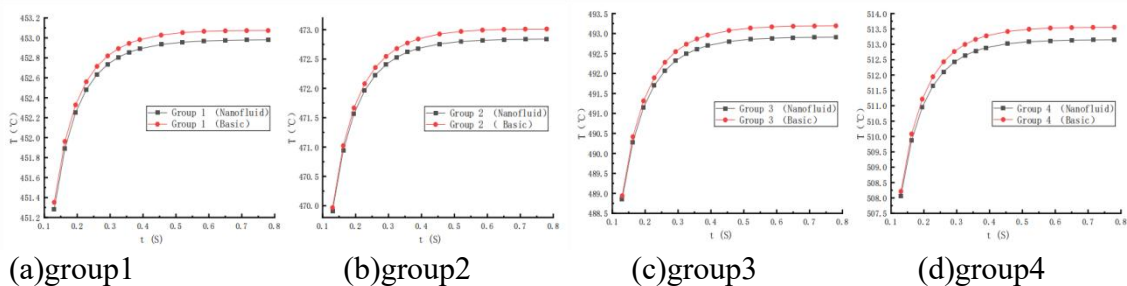


Figure 3.1 Average wall temperature versus time of the evaporation end of the heat pipe at different heat source temperatures

3.2 Effect of porous medium porosity conditions on heat transfer

This paper goes on to simulate the corresponding change of the average wall temperature of the evaporation end and the condensing end of the heat tube using 1% volume concentration of nanofluid under the same boundary conditions and different porosity of the porous medium.

Here, three sets of simulated objects with a porosity of 40%, 50% and 60% at the heat source temperature of $1.2 T_c$ and the cold source temperature of $0.8 T_c$. Specifically, the average wall temperature of the evaporation end and condensing end of the heat pipe was analyzed separately, and a set of data was analyzed every 100 time steps, as shown in Figure 3.2 and Figure 3.3.

As shown in Figure 3.2, the fluid temperature in the heat pipe is equal in the initial stage. When the heat transfer proceeds to 0.4 seconds, the average wall temperature at the evaporation end of the

three porosity heat pipes is in dynamic equilibrium. Among them, the average wall temperature of the evaporation end of the heat pipe with a porosity of 40% rises most rapidly, and the average wall temperature is the highest after stabilization. According to Figure 3.3, the fluid temperature in the heat pipe is equal in the initial stage. When the heat transfer proceeds to 0.4 seconds, the average wall temperature of the condensing end of the heat pipe of the three porosity is in dynamic equilibrium. The average wall temperature of the condensing end of the heat tube with 60% of pores drops most slowly, and the average wall temperature is the highest after stabilization. In conclusion, the average wall temperature of the evaporation end and the condensing end is the minimum after stability, and the temperature uniformity is the best.

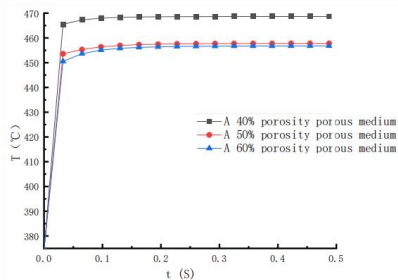


Figure 3.2 Evaporative

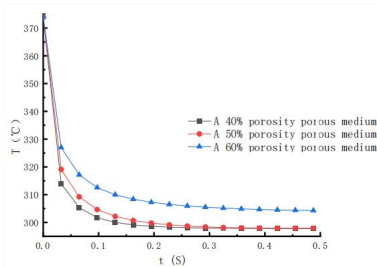


Figure 3.3 Condensation

3.3 Vortex structure

Observation of the regional flow field of heat tube shows the fluid flow in porous medium

Structure, which is a laminar structure in the unconventional sense. In order to analyze the reasons in detail, this chapter, using 1% volume concentration of nano fluid as the tested fluid medium, the porosity of porous media into three groups: 40%, 50% and 60%, respectively tested the fluid inside the porous medium, the results of the nano fluid flow through the porous medium area also appeared vortex structure, the streamline diagram is shown in Figure 5.15.

The test results show that the vortex structures with 60% porosity and 40% are more than in those with 60% porosity. The vortex phenomenon caused by the porous medium in the suction core region leads to local flow field imbalance.

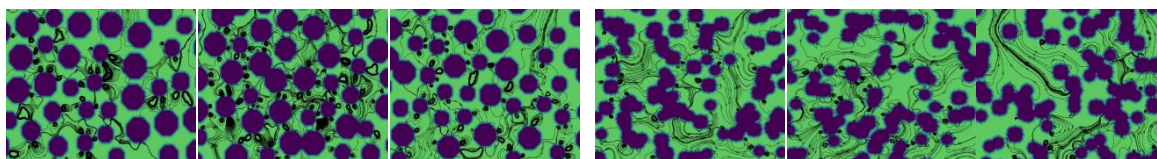


Figure 3.4 Porosity of 40%

Figure 3.5 Porosity of 50%

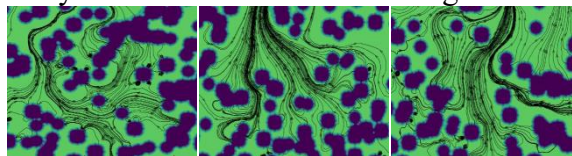


Figure 3.6 Porosity of 40%

4. Conclusion

Here we study the problem of gas-liquid phase transition in heat tubes with nanofluidics as a working medium based on the Boltzmann method combined with the energy equation model. Using the method of combining theory and numerical simulation, it reveals the heat transfer mechanism in the heat pipe, discusses the scientific problems contained therein it, and obtains the following conclusions:

(1) Compared with the base solution, the increase of nanofluid volume concentration and the decrease of particle size can be effective

But the heat transfer performance of the heat pipe is improved, but the change of particle size on the heat transfer performance is less than the change of nanofluid concentration.

(2) The influence of the temperature difference between cold and heat source on the heat transfer performance of the heat pipe is relatively analyzed. The study shows that the higher the heat source temperature, the lower the cold source temperature, the better the heat transfer performance of the heat pipe.

(3) When the fluid flows through the porous medium area, the eddy current structure appears, and the fluid appears more in the porous medium with the porosity of 40% and 50%. The porous medium with porosity of 40%, 50% and 60% was selected to analyze the heat transfer performance of the heat pipe under the same working condition, and the temperature uniformity of the heat pipe with porosity of 60% was the best.

References

- [1] He Wenjie. Boiling and condensation properties of superhydrophilic / superhydrophobic combination surfaces based on the LBM method [D]. Head: Inner Mongolia University of Science and Technology, 2020.
- [2] Shan X, Chen H. Lattice Boltzmann Model for Simulating Flows with Multiple Phases and
- [3] Components [J]. *Physical Review E*, 1993, 47: 1815-1819.
- [4] Zhang C, Cheng P. Mesoscale Simulations of Boiling Curves and Boiling Hysteresis under Constant Wall Temperature and Constant Heat Flux Conditions [J]. *International Journal of Heat and Mass Transfer*, 2017, 110:319-329.
- [5] Gong S, Cheng P. Direct Numerical Simulations of Pool Boiling Curves Including Heater's Thermal Responses and the Effect of Vapor Phase's Thermal Conductivity [J]. *International Communications in Heat and Mass Transfer*, 2017, 87: 61-71.
- [6] Mu Y T, Chen L, He Y L, et al. Nucleate Boiling Performance Evaluation of Cavities at Mesoscale Level [J]. *International Journal Heat and Mass Transfer*, 2017, 106: 708-719.
- [7] Fang W Z, Chen L, Kang Q J, et al. Lattice Boltzmann Modeling of Pool Boiling with Large Liquid-Gas Density Ratio [J]. *International Journal of Thermal Sciences*, 2017, 114: 172-183.
- [8] Liu Jiabin, Zheng Lin, Zhang Beihao. A lattice Boltzmann simulation of the natural convective entropy production of double diffusion in the square cavity of porous medium [J]. *Computational Physics*, 2022, 39 (05): 549-563.
- [9] Yao Jie, Dong Bo, Li Weizhong. Lattice Boltzmann simulation of gas flow through complex microchannels [J]. *Journal of Computational mechanics*, 2022, 39 (05): 641-648.
- [10] Xie Zhenwu, Yang Yiyi, Zou Mingsong. Numerical Research on Rectangular Square Column Based on Grid Boltzmann Method [C] // Collection of the 16th National Hydrodynamics Conference and 32nd National HydroDynamics Symposium (Volume 1), 2021:694-700.
- [11] Xie Chen, Li Yinshan, Huo Shuhao. Square-column winding flow was simulated by the lattice Boltzmann method [J]. *Journal of Hebei University of Technology*, 2021, 50 (04): 17-24.
- [12] Zheng Wenhan, Hong Fangjun. Two-phase closed-loop thermosiphon study based on lattice Boltzmann [J]. *Journal of Engineering Thermophysics*, 2021, 42 (02): 462-467.
- [13] Fang Ning, Shan Yanguang, Yuan Junjie. LBM numerical simulation of droplet spreading and evaporation of different wetting surface processes [J]. *Progress in New Energy*, 2019, 7 (04): 346-353
- [14] Peng Yuan, Laura Schaefer. Equations of state in a lattice Boltzmann model [J]. *PHYSICS OF FLUIDS*, 2006, 18(4): 042101-042111.
- [15] Gong S, Cheng P. A lattice Boltzmann method for simulation of liquid-vapor phasechange heat transfer [J]. *International Journal of Heat and Mass Transfer*, 2012, 55(17-18): 4923-4927.
- [16] Chuangde Zhang, Li Chen, Feifei Qin, Luguo Liu, Wen-Tao Ji, Wen-Quan Tao. Lattice Boltzmann study of bubble dynamic behaviors and heat transfer performance during flow boiling in a serpentine microchannel [J]. *Applied Thermal Engineering*, 2023, 218: 119331.